Volume 1 number 1 January 1974 Nucleic Acids Research

Thermodynamic and kinetic properties of short RNA helices: the oligomer sequence A_nGCU_n

Jeffrey Ravetch, Jay Gralla and D. M. Crothers

Department of Chemistry, Yale University, New Haven, Connecticut 06520

Received 7 November 1973

ABSTRACT

We studied the thermodynamic, kinetic and optical properties of the double helices formed by the series of self-complementary oligonucleotides, $(Ap)_nGpC(pU)_n$, $2 \leq n \leq 4$, and found that the shortest helix, containing just 6 base pairs, is less stable than would be predicted from the properties of the larger molecules. It also shows a markedly smaller hyperchromism on melting than expected. These anomalous properties of a short helix indicate that one cannot always assume that base pair free energies and extinction coefficient changes are independent of helix size.

INTRODUCTION

The ability to predict the secondary structure of an RNA chain of known sequence depends on accurate estimates of the free energy of particular structural features. Recent work has focused on the free energy contribution of base pairs[1-3] and loops of unbonded bases[3-5] It is generally assumed that the conformational free energy consists of an unfavorable term for nucleating the helix by forming the first base pair, and favorable growth free energies for adding subsequent base pairs. These growth free energies depend on base sequence[2,3], but are generally assumed to be independent of helix size.

In the course of our work on the properties of two-stranded double helical oligomers containing mismatched bases in the middle, we found that these molecules had an anomalously small hyperchromism of melting compared to the compound lacking a mismatch[4]. For example, in the series $(Ap)_4G(pC)_N(pU)_4$, the change in extinction coefficient on melting was about twice as large when N = 1 (perfect dimeric double helix) as when N = 2 (one unbonded C on each strand). This means that two helices of length 5 base pairs, separated by mismatched bases, have different pro-

perties from a single helix of ten base pairs. The experiments reported here were designed to follow up on this observation by systematic study of short helices of varying size.

We chose to synthesize and investigate the thermodynamic, kinetic and optical (hypochromic) properties of short RNA dimeric double helices in the series $(Ap)_nGpC(pU)_n$, $1 \leq n \leq 4$. (These molecules will be further abbreviated A_nGCU_n for simplicity). The self-complementarity of this sequence leads to the prediction of antiparallel dimeric double helices; the formation of dimeric complex has been verified for A_4GCU_4[4]. The results of our investigation indicate that there is a distinct anomaly in the stability and hyperchromism of the shorter members of the series. The origin of these effects is not clear, but it is evident that one cannot always assume that the free energy and hypochromism of a base pair stacking interaction are independent of helix size.

MATERIALS AND METHODS

a) Synthesis

The enzymatic synthesis of oligoribonucleotides was performed according to the procedures originally described by Thach and Doty[6] and Martin, et al.[2]. Purity and source of biochemicals, as well as the specific conditions were described in a previous paper[3]. The general synthesis procedure involves random copolymerization of ADP and GDP with crude polynucleotide phosphorylase, followed by cleavage with ribonuclease T_1. The resulting series of oligomers, A_nGp, were separated on TEAE cellulose, and peaks corresponding to A_2Gp, A_3Gp and A_4Gp were identified and purified according to previously described procedures[3]. These products were then treated with alkaline phosphatase to remove the terminal phosphate, preparing them for use as primers in the subsequent reactions. Addition of one C residue was accomplished by the use of primer - dependent PNPase[7,8] and ribonuclease A. The products were separated on TEAE cellulose, treated with alkaline phosphatase and used as primers for the addition of U. Identification of the final products was facilitated by the use of titium labelled UDP

in the final reaction mixture, which allowed unambiguous recognition of the first oligomer peak containing uridine.

b) Measurements

Samples were bound to TEAE cellulose and washed to remove urea, followed by elution with NaCl and desalting by passing the products through Biogel P-2 twice. Samples were then lyophilized and dissolved in buffer I (1M - Na^+, 0.05 M - PO_4^{2-}, 0.475 M - SO_4^{2-}, 1 mM - EDTA, pH 7.0). Little or no loss of material accompanied this technique.

Measurements were carried out on a temperature-jump apparatus (Messanlangenstudiedgesselschaft, Göttingen, W. Germany) modified for double-beam detection, and with the addition of a transient recording device (Biomation, Palo Alto, California) allowing several time scales to be investigated following a single jump. Ultraviolet absorption spectra were obtained with a Cary Model 14 spectrophotometer equipped with a thermostatted cell holder. All samples were dissolved in buffer I. The temperature of the cell in both T-jump and Cary 14 measurements was followed by a calibrated thermistor, with a resultant uncertainty of less than 0.2° C in the solution temperature. Oligomer samples exposed to T-jump measurements were found by paper chromatography to be undegraded.

c) Analysis of Data

The thermodynamic parameters reported here for the oligomer series A_nGCU_n were obtained using the temperature jump technique to resolve the optical components of the melting reaction as previously reported[4]. This procedure has decided advantages over the more common measurement of equilibrium melting curves, because knowledge of the time dependence allows one to measure that portion of the absorbance change that results from conversion of dimeric double helix to random coil. Other processes that contribute to the optical change are temperature dependence of the extinction of the single strand (due to unstacking[8,9]) and of the helix, and "fraying" or unbonding of a few bases at the end of the double helix.

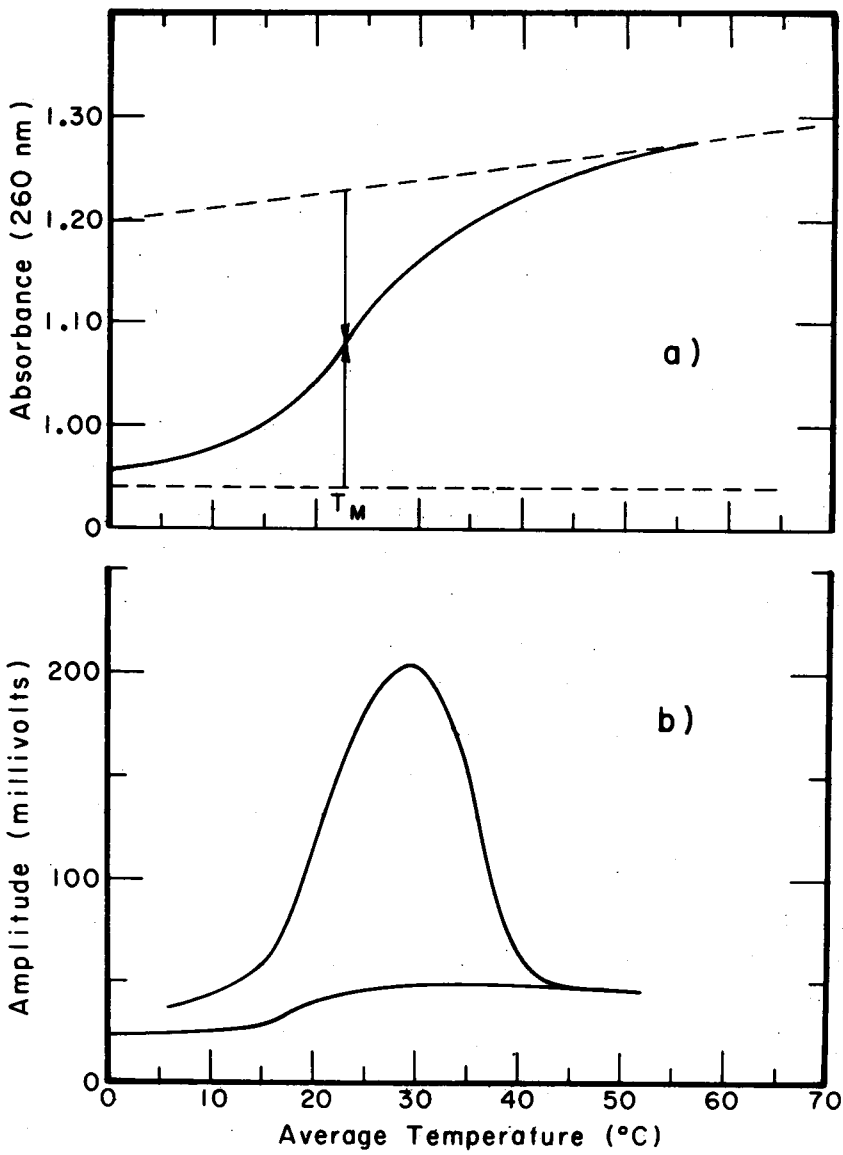

Figure 1: Comparison in method of analysis of thermal transition profiles to yield thermodynamic parameters. a) Spectrophotometric melting profile utilizing flat lower baseline and sloping upper baseline. T_m is defined as the temperature corresponding to the point where the absorbance measured to upper baseline equals the absorbance measured from lower baseline. b) Differential melting profile utilizing partitioning of the absorbance into slow and fast components as revealed through relaxation measurements. T_m is defined as the temperature at which half the slow absorbance change has occurred. See text for further explanation.

Figure 1 shows a schematic comparison of the static and time-resolved methods for determining melting curves. In Figure 1a, the absorbance is measured as a function of temperature, and the absorbance of the single strand is extrapolated back into the transition region. The T_m is usually so low that one cannot accurately measure the temperature dependence of the helix extinction, so this is simply assumed to be independent of temperature. The T_m is the temperature at which the absorbance has risen half way between the two extrapolated lines. In Figure 1b the amplitude of the absorbance change following a temperature jump is plotted as a function of temperature. The upper curve is the total change, and therefore is the derivative of the curve in 1a. The lower line is the portion of the effect that occurs in a few microseconds; the difference between the two is the portion that results from conversion of double helix to single strands. As Figure 1b indicates, and as is found for A_4GCU_4, a fast effect remains even at 0° C where the sample is 99% helix. Therefore the absorbance of the helix is temperature dependent and the flat base line in Figure 1a is incorrect. This leads to small errors in T_m, and substantial errors in such quantities as ΔH which are determined from transition shape.

Transition temperatures, reaction enthalpies and extinction changes were determined from differential melting curves of the type shown in Figure 1b using the equation (1) given by Gralla and Crothers[4]:

$$\Delta H = \frac{4.37 \text{ cal/mole}}{(1/T_{\frac{1}{2}} - 1/T_{\frac{3}{4}})} \qquad (1)$$

where $T_{\frac{1}{2}}$ is the temperature corresponding to maxium absorbance change and $T_{\frac{3}{4}}$ is the temperature at which the absorbance change has dropped to half its maximum value. Corrections for "fraying" from the double helix ends were taken from the same source[4].

RESULTS

a) Thermodynamics of Dimer Formation

We recently reported[4] an investigation of the molecular state of the oligomer series $A_4GC_NU_4$, $1 \leq N \leq 4$, in which sedimentation equilibrium measurements were used to show that dimeric complexes are formed at low temperature. The concentration dependence of the melting temperature and rate of formation were consistent with double helix formation, as expected from the self-complementary base sequence. The compounds in the present series, A_nGCU_n, show closely similar equilibrium and kinetic properties to A_4GCU_4, for which a dimeric complex was established. We therefore interpret our results on A_nGCU_n in terms of double helix formation.

Differential melting profiles for the series A_nGCU_n are shown in Figure 2. These curves were obtained from T-jump measurements which yield two components contributing to the total optical effect. We plotted the difference of the total and fast effects to obtain Figure 3. The temperature corresponding to maximum absorbance change ($T_{\frac{1}{2}}$) is indicative of the relative stability of the molecules when compared at identical concentrations. Two observations should be noted. First, the marked decrease in hyperchromicity in going from A_3GCU_2 is evident, since the peak amplitude decreases dramatically. Second, A_2GCU_2 shows a markedly lower and broader melting profile, indicative of a lower relative stability and enthalpy, when compared to A_3GCU_3 and A_4GCU_4. The relative thermal stability of AGCU could not be accurately determined since at a strand concentration of 180×10^{-6} M its T_m lies below 0° C.

Figure 2: Differential melting profiles for the series A_nGCU_n, n = 2, 3, 4. The total amplitude (-O-O-) is plotted along with the fast amplitude (-●-●-), as obtained from T-jump measurements. The average temperature corresponds to the midpoint of the 4.6° C temperature jump. Data are normalized to $A_{260} = 1.00$. Samples were judged to be chromatographically pure by descending paper chromatography (Whatman 3 MM) developed with 1:1 ammonium acetate: ethanol (vol:vol) by their movement as a single spot. Measurements were done in Buffer I.
a) A_2GCU_2, b) A_3GCU_3 c) A_4GCU_4.

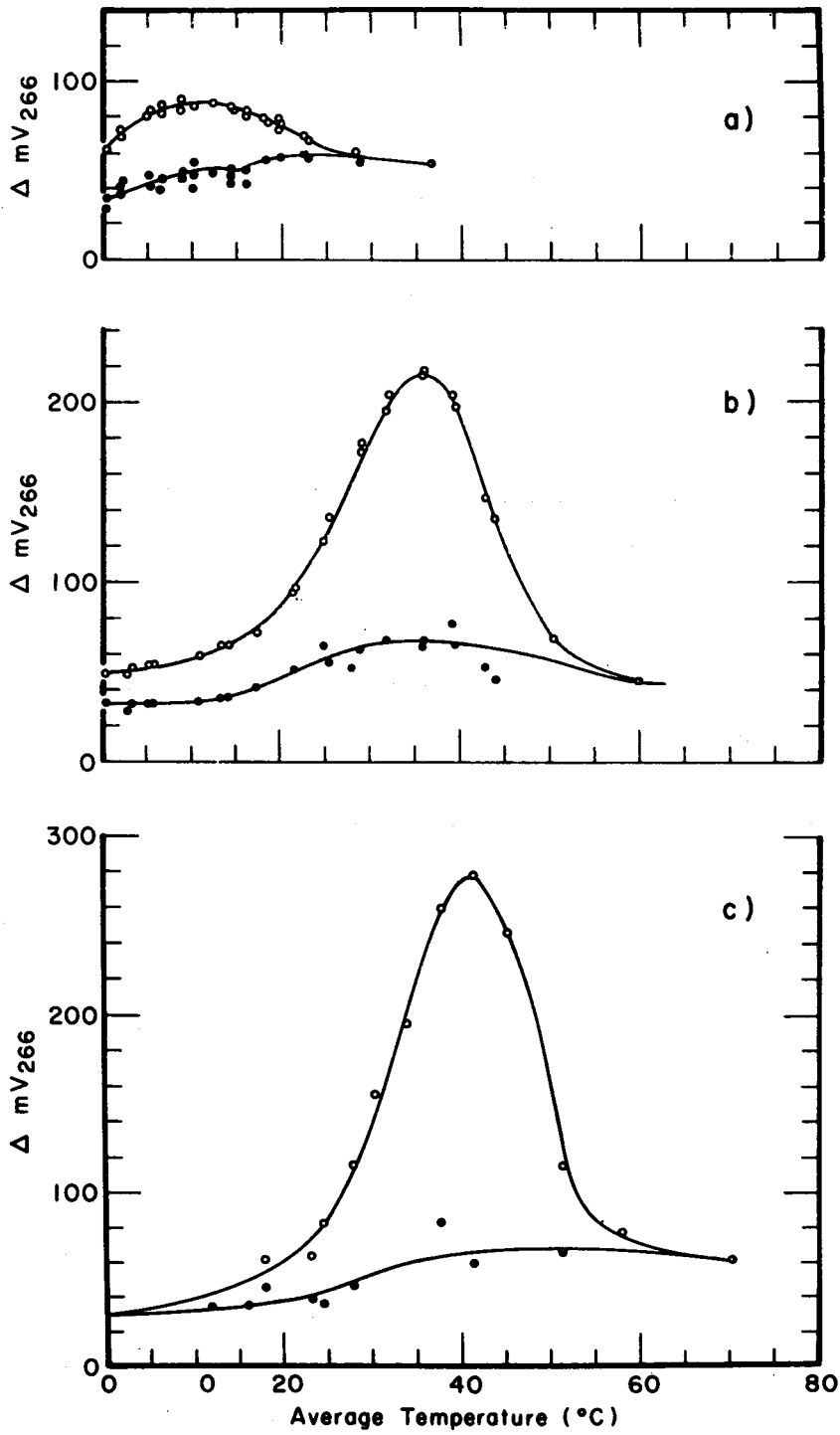
a)
b)
c)
Δ mV266
100
0
200
100
0
300
200
100
0
0
0
20
40
60
80
Average Temperature (°C)

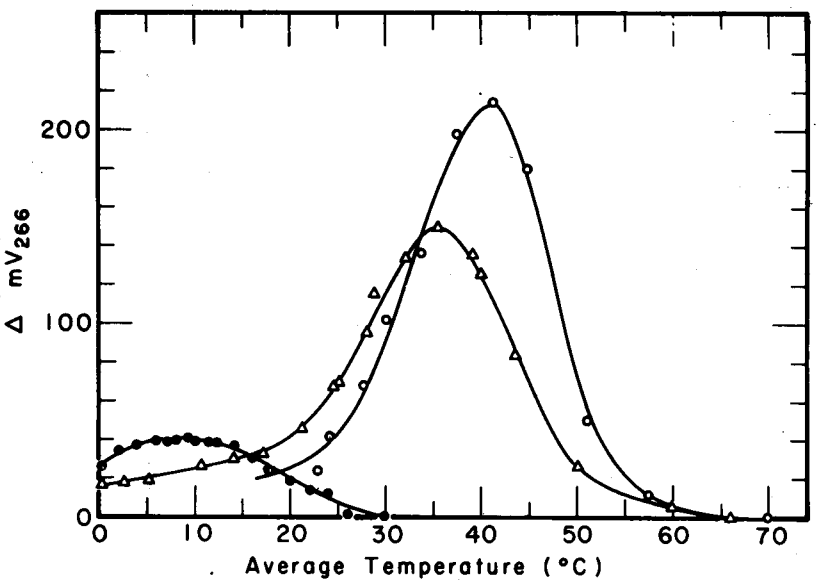

Figure 3: Differential melting profiles for the series A_nGCU_n obtained by subtracting the fast amplitude from the total amplitude (figure 4). Conditions are the same as in figure 4. (-●-●-) A_2GCU_2, (-Δ-Δ-) A_3GCU_3, (-○-○-) A_4GCU_4. Curves reflect only the helix-to-coil transition for these molecules during melting.

TABLE I: Thermodynamic properties of A_nGCU_n, n = 2,3,4 series

Oligomer	T_m(°C)	ΔH(all-or-none) Kcal/mole	ΔH(corrected) Kcal/mole	ΔG loss / pair n → n - 1 25°C Kcal/stack
A_2GCU_2	10° ± 2°	-36 ± 5	-38 ± 5	3 → 2 1.6 ± 0.1
A_3GCU_3	36° ± 1°	-49 ± 5	-57 ± 5	4 → 3 0.95 ± 0.1
A_4GCU_4	42° ± 1°	-59 ± 6	-69 ± 6	

Total concentration (C_T) = 9 x 10^{-6} M in strands, estimated from the absorbance with an average extinction coefficient per nucleotide of 8 x10^3 $M^{-1}cm^{-1}$.

From these curves, enthalpies were calculated according to Equation (1). These values are presented both in their uncorrected form, assuming an all-or-none process, and corrected for fraying[4] in Table I. Plots of $1/T_m$ vs. log total concentration C_T were then constructed using the fact that the equilibrium constant $K = 1/C_T$ at $T = T_m$ and employing the relationship

$$\frac{d \ln K}{d(1/T)} = -\frac{\Delta H}{R} \qquad (2)$$

These results are shown in Figure 4. From this plot one can determine the incremental free energy of helix formation provided by the extra base pairs in going from A_2GCU_2 to A_3GCU_3 to A_4GCU_4. This increment in ΔG is twice the free energy per base pair, and is related to C_T by the equation[3]:

$$\Delta G^{(i)} - \Delta G^{(j)} = RT (\log C_T^{(i)} - \log C_T^{(j)}) \qquad (3)$$

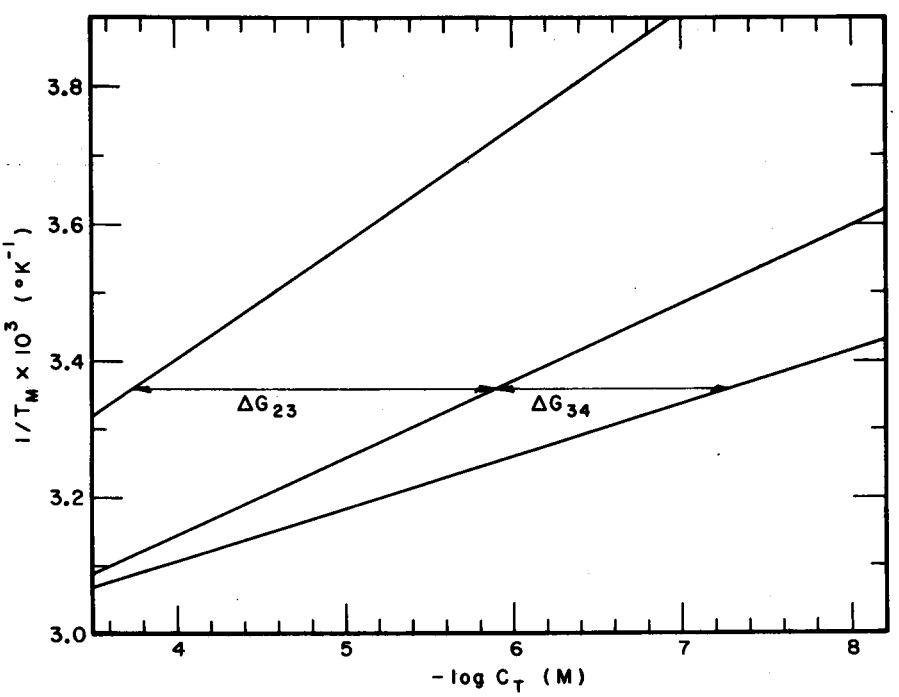

Figure 4: Calculated variation in melting temperature T_m with strand concentration (log C_T) for the series A_nGCU_n. ΔG_{23} corresponds to the free energy loss in going from A_3GCU_3 to A_2GCU_2; ΔG_{34} corresponds to the free energy loss in going from A_4GCU_4 to A_3GCU_3. See text for explanation.

where i and j represent different oligoribonucleotide complexes at a particular temperature. The resultant free energy per A·U stacking interaction is tabulated in Table I. The predicted free energy per A·U stack is 1.1 Kcal at 25° C; this agrees with the experimental increment per A·U pair between A_3GCU_3 and A_4GCU_4. However, the loss of 1.6 Kcal per A·U stack at 25° C in going from A_3GCU_3 to A_2GCU_2 shows anomalous destabilization with decreased helix size.

It is of interest to compare the thermodynamic parameters for this series of molecules with the sequence isomers A_nCGU_n studied by Uhlenbeck et al.[10]. We have replotted their data to obtain $1/T_m$ vs. log C_T plots for the purpose of comparison with our data. We find from T_m values that the series A_nGCU_n shows greater stability than A_nCGU_n in all cases except that of A_2GCU_2. These are presented in Table II. The lower stability of the A_nCGU_n series suggests that the AU-GC stacking interaction is more favorable thermodynamically than the AU-CG stacking interaction. The lower stability of A_2GCU_2 as compared to A_2GCU_2 will be discussed later.

TABLE II: Thermodynamic parameter for the series A_nCGU_n

Oligomer	T_m (° C)	ΔH (Kcal/mole)	ΔG loss/pair n → n - 1, Kcal/stack
A_2CGU_2	16°	-	3 → 2
			1.2
A_3CGU_3	32°	-65	4 → 3
			0.9
A_4CGU_4	39°	-76	

(from data of Uhlenbeck, et al.). Total concentration (C_T) is 2.5×10^{-5} M in strands. ΔH values are dependent upon method of analysis.

In summary, from our thermodynamic data, we have found agreement with expected relative stabilities for A_4GCU_4 and A_3GCU_3, with anomalously low stability for A_2GCU_2.

b) Relaxation Kinetics of Helix Formation

As has been discussed previously[8,9], two effects are observable following a temperature jump on a double helical oligomer. The "instantaneous" (fast) effect could not be resolved with a conventional T-jump apparatus, since it occurs in a time of < 1 μ sec. The second, resolvable effect (slow) is attributed to the helix-to-coil transition. The temperature dependence of the relaxation time is shown in Figure 5, measured over a wide range of temperatures.

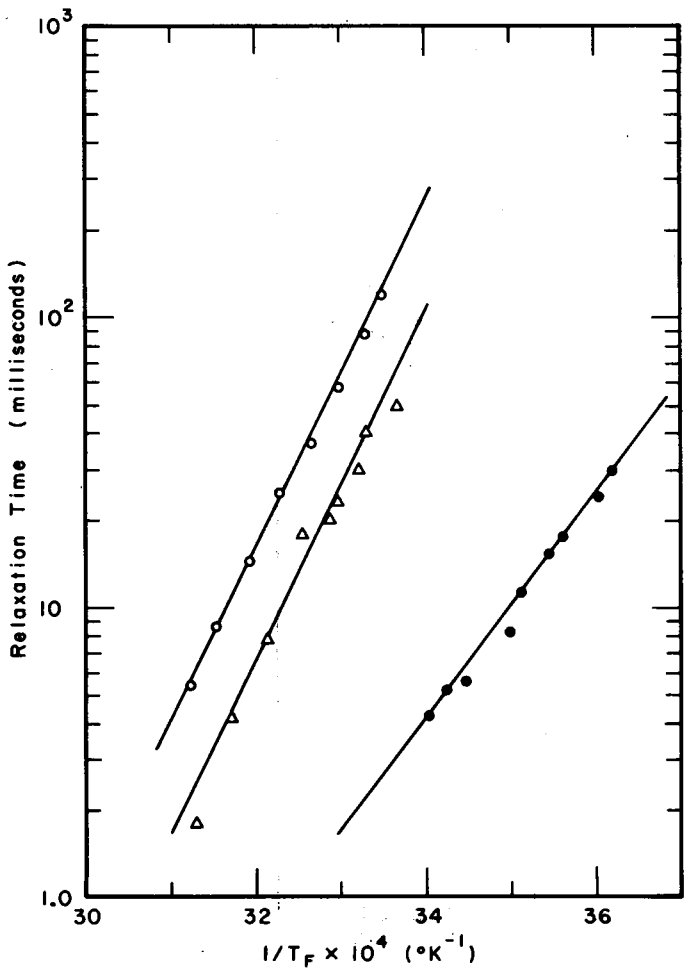

Figure 5: Temperature dependence of the relaxation time τ for the series A_nGCU_n. The relaxation time obtained from T-jump measurements is plotted vs. the reciprocal of the final temperature ($T_{initial}$ + 4.6° C). (-●-●-) A_2GCU_2, (-Δ-Δ-) A_3GCU_3, (-O-O-) A_4GCU_4.

Rate constants for the helix-to-coil transition may be derived from the temperature dependence of the relaxation rate, if the relative concentrations of helix and coil are known at each temperature. The relationship of the forward (k_1) and reverse (k_{-1}) rate constants to the observed relaxation time is:

$$\frac{1}{\tau} = 4 k_1 [C_S] + k_{-1} \qquad (4)$$

where C_S is the free strand concentration. Analysis[4] of the thermal

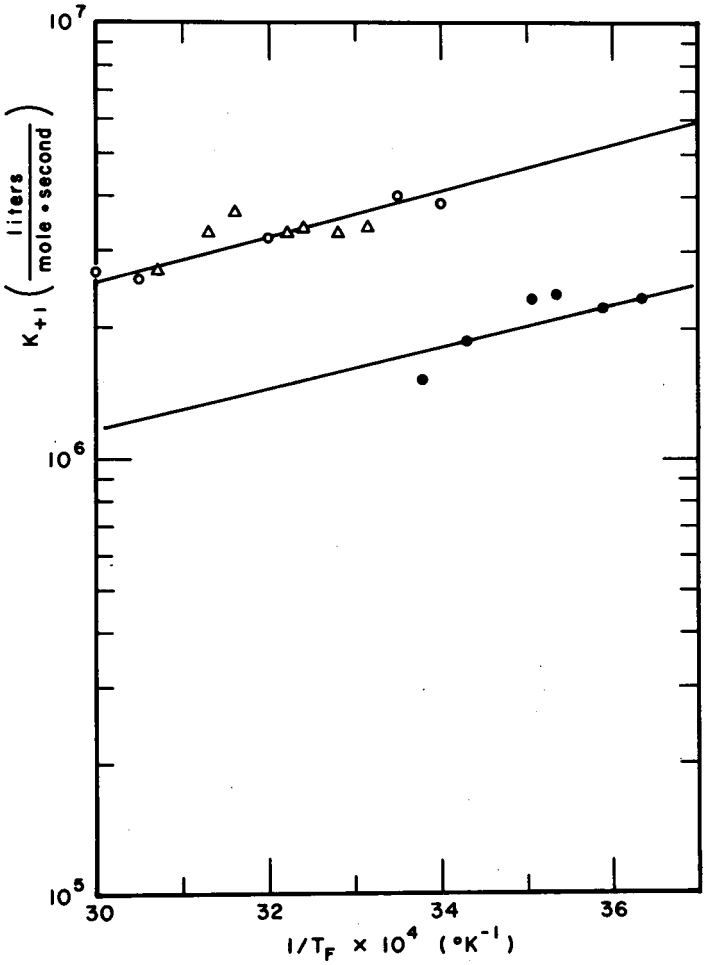

Figure 6: Temperature dependence of the forward rate constant (k_1) for the series A_nGCU_n. Values are plotted against the reciprocal of the final temperature. (-●-●-) A_2GCU_2, (-Δ-Δ-) A_3GCU_3, (-O-O-) A_4GCU_4.

transition profiles leads to accurate values of C_S and the equilibrium constant $K_{eq.}$. Using equation (2) and the measured heat of melting from equation (1), we can obtain $K_{eq.}$ as a function of temperature. Thus, since $K_{eq.} = k_1/k_{-1}$, we can write a simple expression for the reverse rate constant that depends only on an accurate knowledge of the relaxation time τ and the equilibrium constant $K_{eq.}$

$$k_{-1} = \tau^{-1} [4 K_{eq.} C_T(1-\theta) + 1]^{-1} \qquad (5)$$

where θ is the fraction of strands in double helix.

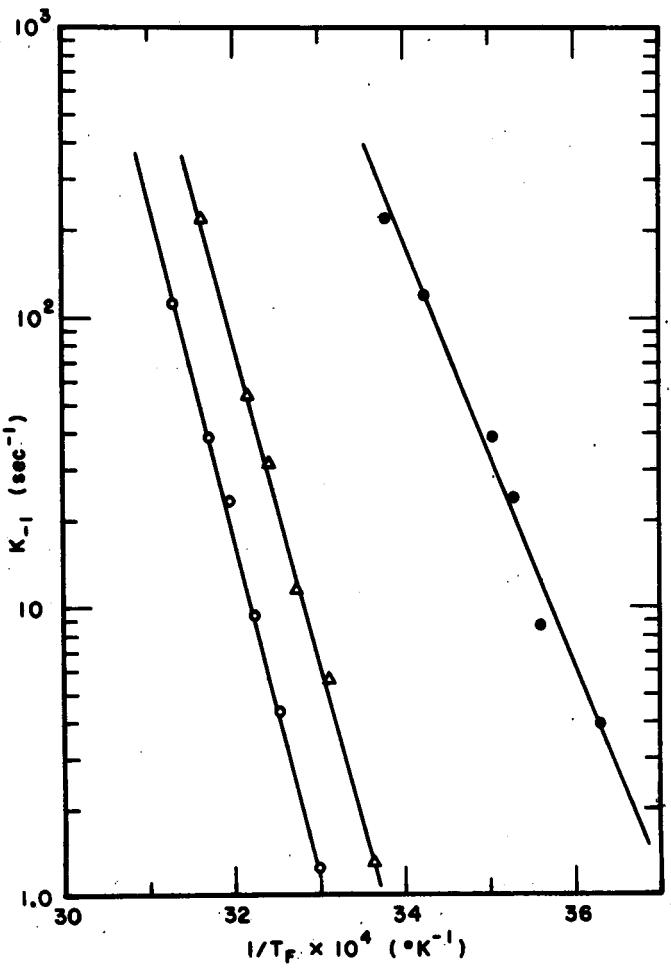

Figure 7: Temperature dependence of the reverse rate constant (k_{-1}) for the series A_nGCU_n. Values are plotted against the reciprocal of the final temperature. (-●-●-) A_2GCU_2, (-Δ-Δ-) A_3GCU_3, (-O-O-) A_4GCU_4.

The temperature dependence of the forward and reverse rate constants are presented in Figures 6 and 7. The bimolecular rate constants for the association of single strands into helices vary from 1×10^6 to 6×10^6 liters per mole of strands per second. A_2GCU_2 shows a consistently slower forward rate constant and faster dissociation constant when compared to A_3GCU_3 and A_4GCU_4.

From these plots we can obtain activation energies according to the Arrhenius equation

$$\frac{\partial \ln k}{\partial (1/T)} = \frac{-E}{R} \qquad (6)$$

Table III lists the activation energies obtained by applying this equation to the slopes in Figures 6 and 7. The dissociation energies are large and positive, with magnitudes roughly proportional to the number of stacks that must be broken. The recombination energies are small and negative, as has been found previously for molecules containing only AU pairs [9]. This implies a kinetic mechanism which involves the for-

TABLE III: Forward and reverse activation energies for the series A_nGCU_n

Oligomer	E_a forward (Kcal/mole)	E_a reverse (Kcal/mole)
A_2GCU_2	-3 ±3	+31 ± 3
A_3GCU_3	-3 ± 3	+49 ±5
A_4GCU_4	-3 ±3	+54 ± 5

Figure 8: The variation in hyperchromism as a function of wavelength and temperature for the series A_nGCU_n. Figures were obtained through T-jump measurements, allowing for the partitioning of the slow and fast components. Wavelengths were varied with a monochromator and an interference filter used to minimize stray light. Only the slow component of the amplitude is shown vs. wavelength for different temperatures, one of which corresponds to the T_m for each molecule.
a) A_2GCU_2 T_m 10°
b) A_3GCU_3 T_m 36°
c) A_4GCU_4 T_m 42°

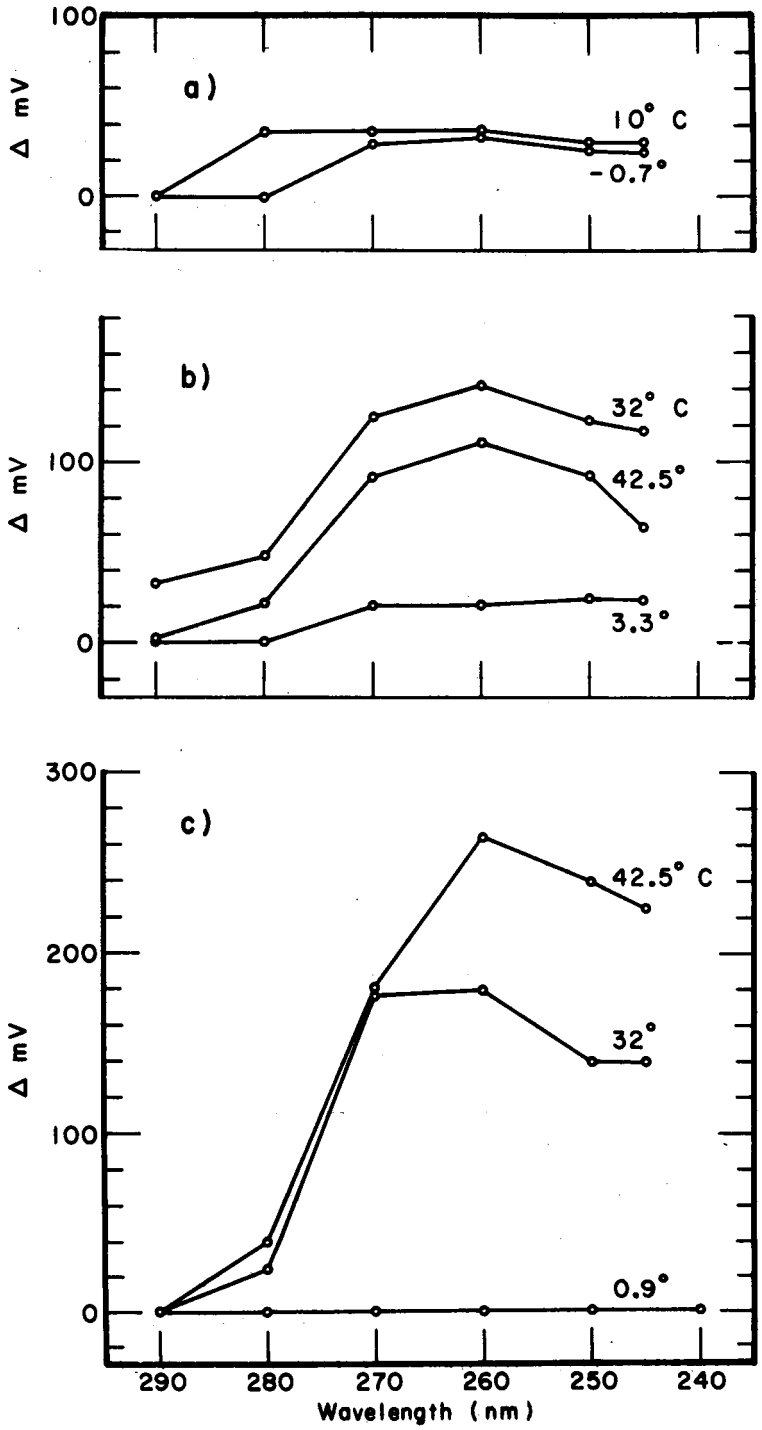
a)
10° C
-0.7°
b)
32° C
42.5°
3.3°
c)
42.5° C
32°
0.9°
Δ mV
100
0
300
200
290
280
270
260
250
240
Wavelength (nm)

mation of a steady-state intermediate with a few bases paired.

c) Hyperchromicity

The variation in amplitude observed during the melting of RNA oligomers has been investigated as a function of wavelength, base composition and temperature for the series A_nGCU_n. Figure 8 shows the dependence of the slow relaxation amplitude on sequence, wavelength and temperature. The difference in extinction between helix and coil can be calculated from the relaxation amplitude using the equation[4]:

$$\epsilon_H - \epsilon_C = \frac{R \left[\frac{d\ \epsilon\ slow}{d\ (1/T)}\right]_{max}}{0.172\ \theta_B\ \Delta H'} \qquad (7)$$

We have defined the terms of this equation previously[4]. Extinction changes at representative wavelengths are given in Table IV. It is evident that the hypochromism changes much less dramatically with oligomer size for λ = 280 nm than for the other wavelengths.

TABLE IV: Extinction coefficient difference, coil minus helix, for A_nGCU_n at several wavelengths.

n	T, °C	λ, nm			
		280	266	260	245
2	10°	1.1×10^3	1.2×10^3	1.2×10^3	1.0×10^3
3	36°	1.7×10^3	5.4×10^3	5.1×10^3	4.2×10^3
4	42°	1.7×10^3	9.2×10^3	10.8×10^3	8.8×10^3

Coefficients $\Delta\epsilon$ are expressed in terms of the molar single strand concentration, and have units $M^{-1}\ cm^{-1}$.

DISCUSSION

The results reported show that the shortest member of the A_nGCU_n series which could be reliably investigated, A_2GCU_2, has anomalous thermodynamic and optical properties. The thermodynamic anomalies are expressed in the standard molar free energy of double helix formation from the single strands. This quantity is 3.2 Kcal less for A_2GCU_2 than for A_3GCU_3 at 25° C. Its expectation value, based on 1.1 Kcal per A·U - A·U stacking interaction found as an average for several oli-

gomers, is 2.2 Kcal. This predicted value is reasonably close to the value of 1.9 found for the difference in standard free energy of formation of A_3GCU_3 and A_4GCU_4. The enthalpy of helix formation does not show an anomalous change for n = 2 within the error margin of the data.

The kinetic results show only a small anomaly for A_2GCU_2 compared to A_3GCU_3 and A_4GCU_4. The association rate constant is smaller by about a factor of two for A_2GCU_2 than for the other two oligomers. According to the thermodynamic results, the equilibrium constant K for forming A_2GCU_2 is about six times smaller than expected based on the properties of A_3GCU_3 and the expected free energy contribution per A·U - A·U stacking interaction. Hence the dissociation rate constant is larger by a factor three than would be expected. These considerations indicate that the source of the anomalously small value of K is about equally divided between association and dissociation rate constants.

The most striking anomaly is to be found in the optical properties of the smallest helix. The $\Delta\epsilon$ values collected in Table IV deserve further comment in this context. Since $\Delta\epsilon$ is expressed in terms of strand molarity, some decrease in $\Delta\epsilon$ is expected as helix size decreases. However, at 260 and 245 nm, $\Delta\epsilon$ decreases by nearly an order of magnitude as the helix size decreases from 10 to 6 base pairs. It should be noted that $\Delta\epsilon$ is more nearly independent of helix size at 280 nm, a wavelength where the contribution comes primarily from the G·C pairs[11]. Evidently the optical properties of the G·C pairs are not as strongly dependent on chain length as those of the A·U pairs, possibly because the former are located at the middle of the double helix.

A common simple assumption[12, 13] is that the hypochromism of a nucleic acid depends on the number of stacking interactions. We find no way to accommodate the data in Table IV to this assumption, without arbitrarily assuming that the number of stacking interactions is less than the expected number of base pairs minus 1.

In summary, the thermodynamic, kinetic and optical properties of A_2GCU_2 do not follow accurately from projections based on the properties of A_3GCU_3 and A_4GCU_4. The final question, which we cannot

answer, is the source of these anomalies. It is natural to ask whether A_2GCU_2 has been correctly identified. The procedures for its synthesis and identification were identical to those for A_3GCU_3 and A_4GCU_4; careful checking revealed no ambiguities. If an error were made, it would have to be in the direction of a molecule with only four base pairs, such as A_2GCU. We synthesized AGCU, and found this double helix decidedly less stable than our sample of A_2GCU_2. Hence it is very unlikely that A_2GCU_2 has been incorrectly identified and actually contains only four base pairs.

The anomalous thermodynamic, kinetic and optical properties of A_2GCU_2 must arise from unexpected properties either of the double helix or the single strand. If the single strand could form a specific structure, for example, this could lead to a lowered relative stability of the double helix and to a smaller $\Delta\epsilon$ between the two states. This idea is marginally supported by the kinetic results, since the association rate constant is reduced by a factor 2 from the value for A_3GCU_3. However, we found no unusual relaxation amplitudes for the single strand unstacking effects in and above the melting transition. It therefore seems more likely that the low stability and $\Delta\epsilon$ values are a specific property of the short double helix size.

We should note that most RNA fragments yet studied in which short helices (six base pairs or less) are present contain mostly G·C base pairs. tRNA and its fragments are examples[14-17]. In these cases we have been successful in predicting stability from the properties of model oligomers[15], and there are no indications that the hypochromism is anomalously small. It is therefore possible that the anomalous effect of helix size will be confined to predominantly A·U - containing helices.

Since we cannot offer a definitive interpretation of the source of the helix-size effects, we will not list the possibilities that have occurred to us. The crucial question is whether there are structural anomalies in the shorter helices; this we hope to answer with nuclear magnetic resonance experiments currently in progress.

REFERENCES

1 Tinoco, I., Uhlenbeck, O.C. and Levine, M.D. (1971) Nature 230, 362-367.
2 Martin, F.H., Uhlenbeck, O.C. and Doty, P. (1971) J. Mol. Biol. 57, 201-215.
3 Gralla, J. and Crothers, D.M. (1973a) J. Mol. Biol. 73, 497-511.
4 Gralla, J. and Crothers, D.M. (1973b) J. Mol. Biol. 78, 301-319.
5 Uhlenbeck, O.C., Borer, P.N., Dengler, B. and Tinoco, I. (1973) J. Mol. Biol. 73, 483-496.
6 Thach, R.E. and Doty, P. (1965) Science 148, 632-634.
7 Fitt, P.S. and Fitt, F.A. (1967) Biochem. J. 105, 25-33.
8 Klee, C.B. and Singer, M.F. (1967) Biochem. Biophys. Res. Comm. 41, 1590-1596.
9 Craig, M.E., Crothers, D.M. and Doty, P. (1971) J. Mol. Biol. 62, 383-401.
10 Uhlenbeck, O.C., Martin, F.H. and Doty, P. (1971) J. Mol. Biol. 57, 217-229.
11 Felsenfeld, G. (1971) in Procedures in Nucleic Acid Research, Vol. 2, pp.223-244, Harper and Row, New York.
12 Applequist, J. (1967) in Conformation of Biopolymers, Vol. 1, pp.403-425, Academic Press, London and New York.
13 Scheffler, I.E., Elson, E.L. and Baldwin, R.L. (1970) J. Mol. Biol. 48, 145-171.
14 Riesner, D., Maass, G., Thiebe, R., Philippsen, P. and Zachau, H.G. (1973) Eur. J. Biochem. 36, 76-88.
15 Crothers, D.M., Cole, P.E., Hilbers, C.W. and Shulman, R.G. submitted for publication.
16 Coutts, S. (1971) Biochim. Biophys. Acta 232, 94-106.
17 Kallenbach, N.R., Ma, R.I., Ofengand, J. and Siddiqui, M.A.Q. (1973) Biopolymers 12, 1203-1221.